THE JOURNAL OF PHYSICAL CHEMISTRY B

Article

pubs.acs.org/JPCB

Polarizable Model for DMSO and DMSO−Water Mixtures

Stephan J. Bachmann and Wilfred F. van Gunsteren*

Laboratory of Physical Chemistry, ETH Zürich, CH-8093 Zürich, Switzerland

ABSTRACT: Starting from a nonpolarizable rigid molecular model for DMSO, a polarizable rigid model for DMSO in the liquid phase is proposed. The molecular polarizability is represented by a charge-on-spring (COS) inducible dipole at the sulfur atom and its polarization is damped for large values of the electric field strength. Some parameters of the model, the partial charge distribution, the polarizability, the value of the electric field at which damping sets in, were varied, and the overall depth and repulsion strength of the Lennard−Jones interactions were scaled with the aim of reproducing the experimental values for the molecular dipole moment, the density, heat of vaporization, and static dielectric constant of liquid DMSO at ambient temperature and pressure. The polarizable DMSO/D model well reproduces the experimental data, such as excess free energy, surface tension, translational, and rotational diffusion, for liquid DMSO. The model is further tested in mixtures with polarizable water models and in mixtures with nonpolarizable DMSO. The latter results suggest that it could serve as model for polarizable cosolvent in aqueous solutions.

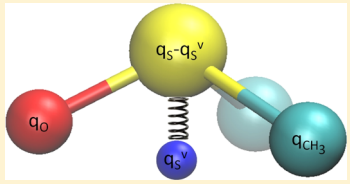

INTRODUCTION

The use of computer simulation to study the behavior of biomolecules such as proteins, nucleic acids, carbohydrates, and lipids at physiological conditions in order to obtain a picture of their conformational and dynamic characteristic features at an atomic level of resolution has shown a steady growth over the past few decades.[1−4] The faithfulness of such simulations depends on the accuracy of the molecular models or force fields used and the extent of sampling of the configurational space that is achieved.[5] Currently, most generally applicable biomolecular force fields treat nonbonded interactions as pairwise additive, and the values of their model or force-field parameters are chosen such that many-body contributions to the nonbonded interactions are included in an average manner.[6−13] For relatively homogeneous systems, such as pure liquids or multicompound systems that contain compounds of similar polarization characteristics, this mean-field approximation of many-body interactions may yield a sufficiently accurate description of system properties. However, for systems containing electronic inhomogeneities, e.g., in the active site of an enzyme or at the surface of a protein or membrane, the explicit introduction of electronic many-body interactions may yield an improved description of system properties. This can be done at the quantum-chemical level of theory[14] or computationally much less costly at the classical level of theory by employing classical induced dipoles,[15,16] either as ideal point dipoles,[17−19] or by allowing atomic charges to fluctuate,[20] or by the introduction of two equal but opposite charges that are kept together by a spring as in the charge-on-spring (COS) model,[21] also called Drude oscillator[22] or shell[23] model. Because of its simplicity with respect to the calculation of the forces, the COS model has been chosen for the introduction of polarizability into the GROMOS biomolecular force field and software.[24,25]

It is long known that the properties of the solvent around a biomolecule play a critical role with respect to its dominant conformation, as is illustrated by the use of cosolvents of water such as salts or urea to induce protein denaturation. Other cosolvents of water such as chloroform or dimethyl sulfoxide (DMSO) are used to increase the solubility of hydrophobic compounds. Water−DMSO mixtures are also used as cryoprotective agent due to their low freezing temperature. Thus, the development of models for water and its cosolvents that are compatible with the general biomolecular force fields is as important as the latter themselves: the key to solve the protein folding lies in an accurate description of the denatured state.[26,27]

The nonideal properties of water−DMSO mixtures have been inferred from a range of experimental measurements,[28−43] see also refs 44 and 45. These offer a challenge to theoretical modeling of this nonideal behavior. During the past decades, a variety of models for DMSO in the condensed phase have been proposed.[39,44−56] They can be classified using different criteria, for example rigid, nonpolarizable models,[39,46−51] or flexible nonpolarizable models[52−55] or polarizable models,[44,45] all treating DMSO at the atomic level of resolution, or supramolecular polarizable models.[56] In the latter model, two DMSO molecules are represented by a coarse-grained (CG) bead consisting of two particles connected by a quartic spring that makes the model polarizable.[56] The model is computationally more efficient, 1−2 orders of magnitude more than atomic models. It describes some properties of CG water−DMSO mixtures even better than atomic level models, compare ref 56 with refs 44 and 45. Yet, its dielectric permittivity $\varepsilon(0)$ is too low, its diffusion too high, its heat capacity too low and its thermal expansion coefficient and compressibility too large[56] compared to experiment. This is the price to be paid for making a model simpler and faster in calculations. The other polarizable

Received: April 11, 2014
Revised: July 30, 2014
Published: August 5, 2014

   dx.doi.org/10.1021/jp5035695 | J. Phys. Chem. B 2014, 118, 10175−10186

model for DMSO[44,45] is of fluctuating-charge type and is compatible with the fluctuating-charge polarizable TIP4P-FQ water model.[20] This makes this model unsuitable for use in conjunction with the GROMOS force field for biomolecules and their solvents.

In the present study, we investigate the possibility to introduce COS polarizability into the GROMOS compatible nonpolarizable model for DMSO.[50] To keep the computational effort required low, only one polarizable COS site is introduced per DMSO molecule. The nonbonded interaction parameters are calibrated using thermodynamic and dielectric properties of the liquid. Mixtures of polarizable DMSO with polarizable water, the COS/G2 model,[57] are simulated and their properties are compared with experimental data. In order to investigate the compatibility of the DMSO models at different levels of resolution, mixtures of atomic nonpolarizable and polarizable DMSO are simulated. The overall goal is to improve the dielectric permittivity and polarization and dynamical properties of the nonpolarizable GROMOS compatible DMSO model without loosing its properties that already agree with experiment.

METHODS

Simulation Setup. The simulations were performed with the GROMOS simulation package.[24,25,58−60] The cubic computational box, with a box length of about 4 nm, contained 512 DMSO molecules. Minimum image periodic boundary conditions were applied. The bond lengths and the bond angles were constrained using the SHAKE algorithm,[61] with a relative geometric tolerance of 10^{-4}, allowing for a time step of 2 fs. Long-range electrostatic interactions were handled with a triple-range cutoff scheme, with cutoff radii of 0.8 nm (interaction updated every time step) and R_c = 1.4 nm (interaction updated every five time steps). The mean effect of omitted electrostatic interactions beyond the long-range cutoff distance was accounted for by the inclusion of a Barker−Watts reaction-field force,[62,63] using a relative permittivity ε_{rf} = 46 for the dielectric continuum beyond the reaction-field radius $R_{rf} = R_c$. To determine the nonbonded pairs, a standard pairlist algorithm was used. Temperature and pressure were kept constant using the weak-coupling method,[64] with coupling times τ_T = 0.1 ps, τ_p = 0.5 ps, and an isothermal compressibility of 4.575×10^{-4} kJ^{-1}mol nm^3. The system was equilibrated for 1 ns at 298.15 *K* and 1 atm before the next 10 ns were used for analysis. During the simulations, every 1000 steps the center of mass motion and rotation of the system were removed. The energies and atom positions were saved every 0.5 ps for analysis.

Binary Mixtures. Mixtures between molecules described by the new polarizable DMSO model and two different water models, the nonpolarizable SPC model[65] and the polarizable COS/G2 model,[57] were simulated. For testing the compatibility between the polarizable and nonpolarizable DMSO models mixtures of these compounds were simulated too. For all three binary mixtures 11 different mixtures from pure polarizable DMSO to pure water or nonpolarizable DMSO with the step size of the mole fraction x equal to 0.1. The simulation boxes contained 1000 molecules. The values of the dielectric permittivity beyond the cutoff radius and of the isothermal compressibility are linear combinations of the experimental values of these properties for the pure liquids.

Analysis of the Simulated Ensembles. The definitions and computational procedures used to obtain the various properties reported can be found in ref 50 and in ref 25. The local mole fraction of component i of a binary mixture consisting of components i and j is defined as follows:

$$x_{ij}(r) = \frac{n_{ii}(r)}{n_{ij}(r) + n_{ii}(r)} \tag{1}$$

where $n_{ij}(r)$ is the number of molecules of type j around a molecules of type i within distance r,

$$n_{ij}(r) = \int_0^r \frac{N_j}{V} g_{ij}(r') 4\pi r'^2 dr' \tag{2}$$

with N_j being the number of molecules of type j in the computational box of volume V, and the following:

$$g_{ij}(r) = \frac{1}{4\pi r^2 dr} \frac{1}{N_m} \left\langle \sum_{i=1}^{N_m} \sum_{j\neq i}^{N_m} 1 \right\rangle \tag{3}$$

is the radial distribution function, with N_m the number of molecules in the box and ρ the density. The heat of mixing ΔH_{mix} can be estimated from the potential energy of the mixtures (U_{mix}) and of the pure compounds (U_i and U_j), according to the following:

$$\Delta H_{mix} = U_{mix} - (x_i U_i + (1 - x_i) U_j) \tag{4}$$

for composition x_i. The excess free energy ΔF_{exc} was obtained by thermodynamic integration, while the free enthalpy of hydrophobic solvation ΔG_s of an argon atom was obtained by Widom particle insertion. The argon parameters can be found in ref 25. The surface tension was obtained from simulations with 5 times larger box length L_z in the z-direction through time averaging over diagonal elements p_{ii} of the pressure tensor,

$$\gamma = \frac{L_z}{2} \left\langle p_{zz} - \frac{1}{2}(p_{xx} + p_{yy}) \right\rangle \tag{5}$$

For this purpose, five different simulations, with different starting velocities and configurations, with a length of 2 *ns* were averaged to get the surface tension of a system.

The static dielectric permittivity $\varepsilon(0)$ was calculated using the fluctuation of the total dipole moment of the system using the following:

$$(\varepsilon(0) - 1)\left(\frac{2\varepsilon_{rf} + 1}{2\varepsilon_{rf} + \varepsilon(0)}\right) = \frac{\langle \vec{M}^2 \rangle - \langle \vec{M} \rangle^2}{3\varepsilon_0 V k_B T} \tag{6}$$

with ε_{rf} being the reaction-field permittivity, ε_0 the dielectric permittivity of vacuum, k_B the Boltzmann constant, and T the temperature. The Debye relaxation time τ_D was obtained from the normalized autocorrelation function,

$$\theta(t) = \frac{\langle \vec{M}(0) \cdot \vec{M}(t) \rangle}{\langle \vec{M}^2 \rangle} = \exp\left(-\frac{t}{\tau_\phi}\right) \tag{7}$$

and the relation

$$\tau_D = \frac{2\varepsilon_{rf} + \varepsilon(0)}{2\varepsilon_{rf} + 1} \tau_\phi \tag{8}$$

for further details, we refer to ref 50 and ref 25.

RESULTS AND DISCUSSION

Parametrization of the Polarizable DMSO/D Model. As a first guess for developing a nonlinear polarizable model the

dx.doi.org/10.1021/jp5035695 | J. Phys. Chem. B 2014, 118, 10175−10186

parameters of the nonpolarizable GROMOS compatible DMSO model[50] were used, see Table 1. The permanent dipole

Table 1. Parameters for the Non-Polarizable DMSO Model of Ref 50 and for the Polarizable DMSO/D Model for DMSO in the Condensed Phase[a]

parameter	DMSO[50]	DMSO/D
no. of interaction sites	4	5
geometry		
d_{SO} [nm]	0.153	0.153
d_{SC} [nm]	0.1937991	0.1937991
θ_{OSC} [degree]	106.75	106.75
θ_{CSC} [degree]	97.4	97.4
damping of polarization		
E_0 [kJ mol^{-1} nm^{-3}]$^{1/2}$]		26
p		8
polarizability		
q^{ν} [e]		−8.0
$\alpha(4\pi\varepsilon_0)^{-1}$ [10^{-3} nm^3]		4.5
atomic charges		
q_S [e]	0.12753	0.080
q_O [e]	−0.44753	−0.38
q_{CH_3} [e]	0.16	0.15
μ^0 [D]	4.51	3.96
Lennard−Jones parameters		
C_6(S) [(kJ mol^{-1} nm^6)$^{1/2}$]	0.10277	0.107786
C_{12}(S) [10^{-3} (10^{-6} kJ mol^{-1} nm^{12})$^{1/2}$]	4.6366	4.93531
C_6(O) [(kJ mol^{-1} nm^6)$^{1/2}$]	0.047652	0.049978
C_{12}(O) [10^{-3} (10^{-6} kJ mol^{-1} nm^{12})$^{1/2}$]	0.86686	0.92271
C_6(CH_3) [(kJ mol^{-1} nm^6)$^{1/2}$]	0.098050	0.102836
C_{12}(CH_3) [10^{-3} (10^{-6} kJ mol^{-1} nm^{12})$^{1/2}$]	5.1620	5.49456

[a]The parameter definitions can be found in refs 25 and 67.

μ^0 of this rigid DMSO molecule is 4.51 D. We note that the value of 5.25 D quoted in ref 50 for this model is wrong, because it results from the assumption that the rigid DMSO molecule is planar. The model of ref 50 is nonplanar though, because the three bond angles θ centered at the sulfur atom add up to 311°. From the simulated ensembles the density ρ, heat of vaporization ΔH_{vap}, various contributions to the potential energy U, induced molecular dipole μ^{ind}, and dielectric permittivity $\varepsilon(0)$ were calculated to evaluate the model. The experimental values for the heat of vaporization, dielectric permittivity and density ρ were the primary targets of the parameter calibration. These properties can be calculated from a single simulation of about 5 ns. For the best model obtained, called the DMSO/D model, other properties given in Table 2 that require a much larger computational effort, were calculated to fully characterize the DMSO/D model.

In a first step, simulations were performed with the values of the molecular polarizability α centered at the sulfur atom ranging from 0.003 to 0.008 $(4\pi\varepsilon_0)$ nm^3, the gas phase value.[66] Using the charges from the nonpolarizable model the dielectric permittivity was too large. The introduction of a sublinear polarizability[67] beyond an electric field strength E_0 to decrease $\varepsilon(0)$ did not help. Therefore, the charge distribution of the DMSO model was changed in such a way that the vacuum experimental permanent dipole moment of 3.96 D of the molecule was maintained. The oxygen charge was changed from −0.45 e up to −0.36 e in steps of 0.01 e, see Table 3. Even using a polarizability α = 0.0045 $(4\pi\varepsilon_0)$ nm^3 the dielectric permittivity was still too large. So the damping of the polarization was increased by lowering the value of the electric field for which the polarization becomes sublinear from E_0 = 40 (kJ mol^{-1} nm^{-3})$^{1/2}$ to 30 (Table 4) and 20 (kJ mol^{-1} nm^{-3})$^{1/2}$ (Table 5). This brought $\varepsilon(0)$ close to the experimental value of 47, but resulted in a too low heat of vaporization. Variation of the polarizability α did not solve this problem, see Table 6. The next step was to vary the depth ε_{LJ} of the Lennard−Jones interaction for all atom pairs. An increase of ε_{LJ} would increase the heat of vaporization without affecting $\varepsilon(0)$ much, see Table 7. Next we performed fine-tuning of the charge distribution and ε_{LJ} for two values of the damping parameter E_0 = 26 (kJ mol^{-1} nm^{-3})$^{1/2}$ (Table 8) and E_0 = 28 (kJ mol^{-1} nm^{-3})$^{1/2}$ (Table 9). The trends observed led to a final fine-tuning of the model by varying the Lennard-Jones C_{12} parameters for all atom pairs, see Table 10. On the basis of these data, the parameters of the resulting DMSO/D model were chosen. They are given in Table 1 and the properties of the DMSO/D model are presented in Table 2.

Evaluation of the Polarizable DMSO/D Model. In Table 2 are shown various properties for the polarizable DMSO/D model and the nonpolarizable model of ref 50. The density, a property against which both models were parametrized, is in perfect agreement with the experimental value for both models. The experimental heat of vaporization could be reproduced within 0.5%. The slight differences between the current work and ref 50 result from minor differences in simulation setup and length. The contributions to the total potential energy are different for the nonpolarizable and polarizable models. The latter has a lower van der Waals energy, which change is offset by the self-polarization energy, resulting in similar electrostatic energies. The excess free energy is slightly smaller than measured in experiment but still within about 1 kJ mol^{-1}. The surface tension of the DMSO/D model is with 45.9 mN m^{-1} slightly larger than the experimental value of 42.7 mN m^{-1} and the value of 43.0 mN m^{-1} obtained for the nonpolarizable model. The average dipole moment of the polarizable DMSO molecule is with 4.46 D slightly smaller than 4.51 D of the nonpolarizable one. The DMSO/D model yields a value of 45 for the dielectric permittivity. This is closer to the experimental value than for the nonpolarizable model. The Debye relaxation time is with 14 ps slightly shorter for the polarizable model than for the nonpolarizable one. The diffusion is for both models a bit faster than in experiment, but still in a good agreement, and so is the rotational relaxation time τ_2^{SO} of the S—O vector. The nonpolarizable DMSO model shows slightly faster tumbling than the DMSO/D model. The secondary thermodynamic quantities C_p, α_p are similar for both models and in reasonable agreement with experiment. The isothermal compressibility is for the polarizable DMSO model smaller than the experimental value and the value for the nonpolarizable model. Both models represent the various properties of the DMSO liquid at 298.15 K and 1 atm rather well, with an improved value for the dielectric permittivity $\varepsilon(0)$ by the DMSO/D model.

Binary Mixtures. The local mole fractions of like molecules in binary mixtures of polarizable DMSO with polarizable and nonpolarizable water are shown in Figure 1 and with nonpolarizable DMSO in Figure 2. Figure 1 shows relatively homogeneous mixing of DMSO and water. The mixture of

dx.doi.org/10.1021/jp5035695 | J. Phys. Chem. B 2014, 118, 10175−10186

Table 2. Liquid State Properties of DMSO (Left) and Water (Right) at 1 atm and 298.15 K As Obtained from Experiment, And for the Non-Polarizable Model[50] as Reported in the Literature and Calculated Here, and for the Polarizable Model DMSO/D[a]

	DMSO				water		
		non-polarizable		polarizable		non-polarizable	polarizable
properties	exp	DMSO[50]	DMSO [this work]	DMSO/D	exp	SPC[25]	COS/G2[25]
ρ [kg m^{-3}]	1095[68]	1096	1096	1096	997[69]	973	999
ΔH_{vap} [kJ mol^{-1}]	52.9[68]	52.9	53.1	52.6	44.05[70]	43.9	43.7
U^{pot} [kJ mol^{-1}]			−50.6	−50.2	−41.5[71]	−41.6	−41.6
U^{CRF} [kJ mol^{-1}]			−19.2	−19.1		−48.6	−68.6
U^{LJ} [kJ mol^{-1}]			−31.4	−34.4		7.0	11.1
$U^{self-pol}$ [kJ mol^{-1}]				3.36			15.9
ΔF_{exc} [kJ mol^{-1}]	29.7[68]	30.5	30.7	28.9	24.0[72]	23.6	21.8
γ [mN m^{-1}]	42.7[73]		43.0	45.9	71.6[74]	48.4	59.0
ΔG_S [kJ mol^{-1}]			5.8	5.6	8.4[75]	8.3	9.6
μ^0 [D]	3.96[76]	4.51	4.51	3.96	1.86[77]	2.27	1.86
$\langle\mu^{ind}\rangle$ [D]				0.52			0.80
$\langle\mu\rangle$ [D]		4.51	4.51	4.46		2.27	2.61
ε (0)	47.24[68]	38	39.5	44.7	78.4[76]	64.7	96.6
τ_D [ps]			17.9	14.0	8.3[76]	6.9	15.8
$\langle D\rangle$ [10^{-9} m^2 s^{-1}]	0.8[78]	1.1	1.0	0.9	2.3[79]	4.1	2.0
$\langle\tau_2^{SO/OH}\rangle$ [ps]	5.2[80]	4.9	5.4	5.6	1.95[81]	1.9	3.9
C_p [J mol^{-1} K^{-1}]	153[68]	139	139	136	75.3[76]	93.0	107.7
α_p [10^{-3} K^{-1}]	9.3[68]	8.6	8.9	8.3	4.22[82]	9.0	7.0
κ_T [10^{-6} atm^{-1}]	53.2[68]	50.8	50.9	45.4	45.8[82]	47.8	47.8

[a]The definition of the properties can be found in refs 50 and 67. Angular brackets indicate averaging over molecules.

Table 3. Properties of DMSO Models with Polarizability α = 0.0045 $(4\pi\varepsilon_0)$ nm^3 and Damping with E_0 = 40 (kJmol^{-1} nm^{-3})$^{1/2}$ for Different Charge Distributions That Reproduce the Experimental μ^0 Value[a]

q_O	q_S	ρ	ΔH_{vap}	U^{pot}	U^{CRF}	$U^{self-pol}$	U^{LJ}	$\langle\mu^{ind}\rangle$	μ^0	$\langle\mu\rangle$	$\varepsilon(0)$
e	e	kg m^{-3}	kJ mol^{-1}	kJ mol^{-1}	kJ mol^{-1}	kJ mol^{-1}	kJ mol^{-1}	D	D	D	
−0.38	0.0780	1104.3	51.8	−49.33	−22.42	4.56	−31.47	0.73	3.97	4.64	61.3
−0.39	0.1010	1105.1	52.0	−49.59	−22.83	4.73	−31.50	0.74	3.98	4.65	56.5
−0.40	0.1260	1105.8	52.3	−49.83	−23.22	4.92	−31.52	0.74	3.97	4.66	72.7
−0.41	0.1510	1106.2	52.5	−50.09	−23.68	5.11	−31.52	0.75	3.97	4.66	65.1
−0.42	0.1760	1107.1	52.9	−50.43	−24.23	5.33	−31.53	0.76	3.98	4.67	62.6

[a]Density ρ, heat of vaporization ΔH_{vap}, potential energy U^{pot} with its Coulomb plus reaction-field (U^{CRF}), COS self-polarization ($U^{self-pol}$), and Lennard−Jones (U^{LJ}) contributions, induced molecular dipole μ^{ind}, the permanent molecular dipole μ^0, molecular dipole μ, static dielectric permittivity $\varepsilon(0)$. Angular brackets indicate averaging over molecules.

Table 4. Properties of DMSO Models with Polarizability α = 0.0045$(4\pi\varepsilon_0)$ nm^3 and Damping with E_0 = 30 (kJ mol^{-1} nm^{-3})$^{1/2}$ for Different Charge Distributions That Reproduce the Experimental μ^0 Value[a]

q_O	q_S	ρ	ΔH_{vap}	U^{pot}	U^{CRF}	$U^{self-pol}$	U^{LJ}	$\langle\mu^{ind}\rangle$	μ^0	$\langle\mu\rangle$	$\varepsilon(0)$
e	e	kg m^{-3}	kJ mol^{-1}	kJ mol^{-1}	kJ mol^{-1}	kJ mol^{-1}	kJ mol^{-1}	D	D	D	
−0.36	0.0330	1097.2	50.2	−47.71	−19.97	3.59	−31.34	0.59	3.96	4.50	48.0
−0.37	0.0570	1097.7	50.2	−47.79	−20.09	3.68	−31.38	0.59	3.96	4.49	49.5
−0.38	0.0780	1098.5	50.5	−48.05	−20.43	3.79	−31.41	0.59	3.97	4.51	48.5
−0.39	0.1010	1099.1	50.7	−48.27	−20.74	3.91	−31.44	0.59	3.98	4.51	49.0
−0.40	0.1260	1099.7	50.9	−48.45	−21.01	4.03	−31.46	0.59	3.97	4.51	55.7
−0.41	0.1510	1100.3	51.1	−48.69	−21.36	4.16	−31.49	0.60	3.97	4.51	59.4
−0.42	0.1760	1100.5	51.4	−48.95	−21.77	4.31	−31.49	0.60	3.98	4.52	52.9

[a]Density ρ, heat of vaporization ΔH_{vap}, potential energy U^{pot} with its Coulomb plus reaction-field (U^{CRF}), COS self-polarization ($U^{self-pol}$), and Lennard−Jones (U^{LJ}) contributions, molecular dipole μ^{ind}, the permanent molecular dipole μ^0, molecular dipole μ, static dielectric permittivity $\varepsilon(0)$. Angular brackets indicate averaging over molecules.

polarizable with nonpolarizable DMSO is very homogeneous (Figure 2). Figure 3 and Figure 4 show volumetric and energetic data for these mixtures. The properties show smooth behavior as a function of the mole fraction water (Figure 3). The slightly too low density of SPC water is reflected in the mixtures. The ΔH_{mix} and ΔV_{mix} show different behavior for nonpolarizable SPC water and polarizable COS/G2 water, but the maximum values of −1.5 kJ mol^{-1} (SPC), 0.4 kJ mol^{-1} (COS/G2), −0.6 nm^3 (SPC) and +0.2 nm^3 (COS/G2) are small. The polarizable COS/G2 water molecules show slightly

dx.doi.org/10.1021/jp5035695 | J. Phys. Chem. B 2014, 118, 10175−10186

Table 5. Properties of DMSO Model with Polarizability $\alpha = 0.0045\ (4\pi\varepsilon_0)\ \mathrm{nm}^3$ and Damping with $E_0 = 20\ (\mathrm{kJ\ mol^{-1}\ nm^{-3}})^{1/2}$ for Different Charge Distributions That Reproduce the Experimental μ^0 Value[a]

q_O	q_S	ρ	ΔH_{vap}	U^{pot}	U^{CRF}	$U^{self-pol}$	U^{LJ}	$\langle\mu^{ind}\rangle$	μ^0	$\langle\mu\rangle$	$\varepsilon(0)$
e	e	kg m^{-3}	kJ mol^{-1}	kJ mol^{-1}	kJ mol^{-1}	kJ mol^{-1}	kJ mol^{-1}	D	D	D	
−0.38	0.0780	1090.9	49.1	−46.67	−18.15	2.77	−31.29	0.41	3.97	4.34	42.8
−0.39	0.1010	1091.7	49.3	−46.87	−18.38	2.83	−31.33	0.41	3.98	4.34	43.6
−0.40	0.1260	1092.1	49.5	−47.04	−18.58	2.91	−31.36	0.41	3.97	4.34	40.2
−0.41	0.1510	1092.5	49.7	−47.24	−18.83	2.98	−31.39	0.41	3.97	4.34	41.6
−0.42	0.1760	1093.1	49.9	−47.50	−19.16	3.07	−31.41	0.41	3.98	4.34	40.0

[a]Density ρ, heat of vaporization ΔH_{vap}, potential energy U^{pot} with its Coulomb plus reaction-field (U^{CRF}), COS self-polarization ($U^{self-pol}$), and Lennard−Jones (U^{LJ}) contributions, molecular dipole μ^{ind}, the permanent molecular dipole μ^0, molecular dipole μ, static dielectric permittivity $\varepsilon(0)$. Angular brackets indicate averaging over molecules.

Table 6. Properties of DMSO Models with an Oxygen Charge $q_O = -0.38e$ and a Sulfur Charge $q_S = 0.081e$ that Reproduce the Experimental μ^0 Value and Damping with $E_0 = 30\ (\mathrm{kJ\ mol^{-1}\ nm^{-3}})^{1/2}$ for Different Polarisabilities α[a]

$\alpha\ (4\pi\varepsilon_0)^{-1}$	ρ	ΔH_{vap}	U^{pot}	U^{CRF}	$U^{self-pol}$	U^{LJ}	$\langle\mu^{ind}\rangle$	μ^0	$\langle\mu\rangle$	$\varepsilon(0)$
[nm^3]	kg m^{-3}	kJ mol^{-1}	kJ mol^{-1}	kJ mol^{-1}	kJ mol^{-1}	kJmol^{-1}	D	D	D	
0.0045	1098.5	50.5	−48.05	−20.43	3.79	−31.41	0.59	3.97	4.51	48.5
0.0050	1100.8	50.7	−48.26	−21.21	4.40	−31.45	0.66	3.96	4.56	62.5
0.0055	1103.9	51.0	−48.57	−22.15	5.07	−31.49	0.73	3.96	4.62	56.8
0.0060	1106.8	51.3	−48.86	−23.12	5.78	−31.52	0.80	3.96	4.69	64.5
0.0065	1109.8	51.6	−49.14	−24.13	6.55	−31.55	0.87	3.96	4.76	60.6
0.0070	1112.9	51.8	−49.40	−25.18	7.37	−31.59	0.94	3.96	4.83	79.2
0.0075	1115.6	52.1	−49.61	−26.25	8.24	−31.60	1.01	3.96	4.90	71.6
0.0080	1118.8	52.3	−49.83	−27.36	9.16	−31.63	1.09	3.96	4.96	66.5

[a]Density ρ, heat of vaporization ΔH_{vap}, potential energy U^{pot} with its Coulomb plus reaction-field (U^{CRF}), COS self-polarization ($U^{self-pol}$), and Lennard−Jones (U^{LJ}) contributions, molecular dipole μ^{ind}, the permanent molecular dipole μ^0, molecular dipole μ, static dielectric permittivity $\varepsilon(0)$. Angular brackets indicate averaging over molecules.

Table 7. Properties of DMSO Models with Polarisability $\alpha = 0.0045\ (4\pi\varepsilon_0)\ \mathrm{nm}^3$ and Damping with $E_0 = 30\ (\mathrm{kJ\ mol^{-1}\ nm^{-3}})^{1/2}$ with an Oxygen Charge of $q_O = -0.38\ e$, a Sulfur Charge $q_S = 0.081$ e that Reproduce the Experimental μ^0 Value for Different Scaling Factors $f(\varepsilon_{LJ})$ of the Lennard−Jones Depth Parameter ε_{LJ} for All Atom Pairs[a]

$f(\varepsilon_{LJ})$	ρ	ΔH_{vap}	U^{pot}	U^{CRF}	$U^{self-pol}$	U^{LJ}	$\langle\mu^{ind}\rangle$	μ^0	$\langle\mu\rangle$	$\varepsilon(0)$
	kg m^{-3}	kJ mol^{-1}	kJ mol^{-1}	kJ mol^{-1}	kJ mol^{-1}	kJ mol^{-1}	D	D	D	
0.97	1092.2	49.1	−46.65	−20.25	3.76	−30.17	0.59	3.96	4.49	55.6
0.98	1094.1	49.5	−47.07	−20.27	3.77	−30.57	0.59	3.96	4.49	47.3
0.99	1096.0	49.9	−47.49	−20.28	3.77	−30.98	0.59	3.96	4.49	52.2
1.00	1097.8	50.4	−47.92	−20.30	3.78	−31.40	0.59	3.96	4.49	51.0
1.01	1099.9	50.8	−48.35	−20.32	3.78	−31.82	0.59	3.96	4.49	49.0
1.02	1101.7	51.2	−48.79	−20.34	3.79	−32.24	0.59	3.96	4.49	53.5
1.03	1103.6	51.7	−49.21	−20.35	3.79	−32.66	0.59	3.96	4.49	48.7
1.04	1105.3	52.1	−49.64	−20.36	3.79	−33.07	0.59	3.96	4.49	51.9
1.05	1107.0	52.5	−50.07	−20.38	3.80	−33.49	0.59	3.96	4.49	50.9
1.06	1108.9	52.9	−50.50	−20.39	3.80	−33.91	0.59	3.96	4.49	61.8

[a]Density ρ, heat of vaporization ΔH_{vap}, potential energy U^{pot} with its Coulomb plus reaction-field (U^{CRF}), COS self-polarization ($U^{self-pol}$), and Lennard−Jones (U^{LJ}) contributions, molecular dipole μ^{ind}, the permanent molecular dipole μ^0, molecular dipole μ, static dielectric permittivity $\varepsilon(0)$. Angular brackets indicate averaging over molecules.

insufficient interaction with polarizable DMSO/D molecules. This is due to the slightly too strong interaction between polarizable COS/G2 water molecules in the liquid phase. Indications for the latter are the too large free enthalpy of hydrophobic hydration ΔG_s and the too large dielectric constant of COS/G2 water compared to experiment (Table 2). Figure 4 shows that polarizable and nonpolarizable DMSO molecules mix well.

Free energies and dielectric properties for the mixtures are shown in Figure 5 for the binary mixtures of polarizable DMSO/D and polarizable (COS/G2) and nonpolarizable (SPC) water and in Figure 6 for the mixture between polarizable and nonpolarizable DMSO. The mixtures of DMSO with water show a smooth but nonlinear behavior as a function of mole fraction water. The excess free energy of the mixture of the two DMSO models shows a linear increase between the excess free energies for the pure liquids. The surface tension in Figure 5 shows for the mixture of polarizable DMSO/D and polarizable COS/G2 water the same trend as the experimental values. The deviation from experimental values for large mole fraction of water is due to the COS/G2 model underestimating the surface tension of water by 20%, see Table 2. In the mixture of polarizable and nonpolarizable DMSO (Figure 6), the surface tension is decreasing almost

dx.doi.org/10.1021/jp5035695 | J. Phys. Chem. B 2014, 118, 10175−10186

Table 8. Properties of the DMSO Models with Polarisability α = 0.0045 $(4\pi\varepsilon_0)$ nm^3 and Damping with E_0 = 26(kJ mol^{-1} nm^{-3})$^{1/2}$ As a Function of the Oxygen Charge q_O, Sulfur Charge q_S that Reproduce the Experimental μ^0 Value and the Scaling Factor $f(\varepsilon_{LJ})$ of the Lennard–Jones Depth Parameter ε_{LJ} for All Atom Pairs[a]

q_O	q_S	$f(\varepsilon_{LJ})$	ρ	ΔH_{vap}	U^{pot}	U^{CRF}	$U^{self-pol}$	U^{LJ}	$\langle\mu^{ind}\rangle$	μ^0	$\langle\mu\rangle$	$\varepsilon(0)$
e	e		kg m^{-3}	kJ mol^{-1}	kJ mol^{-1}	kJ mol^{-1}	kJ mol^{-1}	kJ mol^{-1}	D	D	D	
−0.360	0.033	1.05	1103.5	51.7	−49.28	−19.17	3.27	−33.37	0.52	3.96	4.43	49.3
−0.360	0.033	1.06	1105.2	52.1	−49.71	−19.19	3.27	−33.79	0.52	3.96	4.43	47.6
−0.360	0.033	1.07	1107.1	52.6	−50.15	−19.21	3.28	−34.21	0.52	3.96	4.43	48.1
−0.360	0.033	1.08	1108.6	53.0	−50.57	−19.22	3.28	−34.62	0.52	3.96	4.43	51.8
−0.360	0.033	1.09	1110.7	53.5	−51.01	−19.24	3.28	−35.06	0.52	3.96	4.43	49.6
−0.360	0.033	1.10	1112.3	53.9	−51.44	−19.25	3.29	−35.47	0.52	3.96	4.43	48.3
−0.370	0.056	1.05	1104.2	51.9	−49.42	−19.35	3.34	−33.42	0.52	3.96	4.43	49.6
−0.370	0.056	1.06	1105.8	52.3	−49.85	−19.36	3.35	−33.83	0.52	3.96	4.43	47.3
−0.370	0.056	1.07	1107.7	52.7	−50.28	−19.38	3.35	−34.25	0.52	3.96	4.43	52.7
−0.370	0.056	1.08	1109.3	53.2	−50.71	−19.40	3.36	−34.67	0.52	3.96	4.43	47.3
−0.370	0.056	1.09	1111.0	53.6	−51.14	−19.41	3.36	−35.09	0.52	3.96	4.43	51.3
−0.370	0.056	1.10	1112.9	54.0	−51.58	−19.43	3.36	−35.52	0.52	3.96	4.43	45.2
−0.380	0.080	1.05	1104.7	52.0	−49.56	−19.53	3.42	−33.46	0.52	3.96	4.43	48.0
−0.380	0.080	1.06	1106.3	52.4	−49.98	−19.54	3.43	−33.87	0.52	3.96	4.43	50.4
−0.380	0.080	1.07	1108.2	52.9	−50.42	−19.56	3.43	−34.29	0.52	3.96	4.43	46.7
−0.380	0.080	1.08	1109.9	53.3	−50.85	−19.57	3.43	−34.71	0.52	3.96	4.43	49.7
−0.380	0.080	1.09	1111.6	53.7	−51.28	−19.59	3.44	−35.13	0.52	3.96	4.43	48.8
−0.380	0.080	1.10	1113.2	54.2	−51.71	−19.60	3.44	−35.55	0.52	3.96	4.43	46.0

[a]Density ρ, heat of vaporization ΔH_{vap}, potential energy U^{pot} with its Coulomb plus reaction-field (U^{CRF}), COS self-polarization ($U^{self-pol}$), and Lennard–Jones (U^{LJ}) contributions, molecular dipole μ^{ind}, the permanent molecular dipole μ^0, molecular dipole μ, static dielectric permittivity $\varepsilon(0)$. Angular brackets indicate averaging over molecules.

Table 9. Properties of the DMSO Models with Polarizability α = 0.0045 $(4\pi\varepsilon_0)$ nm^3 and Damping with E_0 = 28(kJ mol^{-1} nm^{-3})$^{1/2}$ as a Function of the Oxygen Charge q_O, Sulfur Charge q_S that Reproduce the Experimental μ^0 Value and the Scaling Factor $f(\varepsilon_{LJ})$ of the Lennard–Jones Depth Parameter ε_{LJ} for All Atom Pairs[a]

q_O	q_S	$f(\varepsilon_{LJ})$	ρ	ΔH_{vap}	U^{pot}	U^{CRF}	$U^{self-pol}$	U^{LJ}	$\langle\mu^{ind}\rangle$	μ^0	$\langle\mu\rangle$	$\varepsilon(0)$
e	e		kg m^{-3}	kJ mol^{-1}	kJ mol^{-1}	kJ mol^{-1}	kJ mol^{-1}	kJ mol^{-1}	D	D	D	
−0.360	0.033	1.05	1104.9	52.0	−49.55	−19.60	3.45	−33.40	0.55	3.96	4.46	49.7
−0.360	0.033	1.06	1106.7	52.4	−49.98	−19.62	3.45	−33.82	0.55	3.96	4.46	53.1
−0.360	0.033	1.07	1108.6	52.9	−50.42	−19.64	3.46	−34.24	0.55	3.96	4.46	52.3
−0.360	0.033	1.08	1110.2	53.2	−50.85	−19.65	3.46	−34.66	0.55	3.96	4.46	52.3
−0.360	0.033	1.09	1112.0	53.7	−51.29	−19.67	3.47	−35.08	0.55	3.96	4.46	49.1
−0.360	0.033	1.10	1113.8	54.2	−51.72	−19.69	3.47	−35.50	0.55	3.96	4.46	50.6
−0.370	0.056	1.05	1105.4	52.1	−49.69	−19.79	3.53	−33.43	0.56	3.96	4.47	53.9
−0.370	0.056	1.06	1107.3	52.6	−50.13	−19.81	3.53	−33.86	0.56	3.96	4.47	51.3
−0.370	0.056	1.07	1109.0	53.0	−50.56	−19.82	3.54	−34.28	0.56	3.96	4.47	50.5
−0.370	0.056	1.08	1110.7	53.4	−50.99	−19.84	3.54	−34.70	0.56	3.96	4.47	48.1
−0.370	0.056	1.09	1112.5	53.9	−51.43	−19.86	3.55	−35.12	0.56	3.96	4.47	50.5
−0.370	0.056	1.10	1114.1	54.2	−51.85	−19.87	3.55	−35.54	0.56	3.96	4.47	51.2
−0.380	0.080	1.05	1105.9	52.3	−49.83	−19.98	3.62	−33.47	0.56	3.96	4.47	49.3
−0.380	0.080	1.06	1107.7	52.7	−50.26	−19.99	3.62	−33.89	0.56	3.96	4.47	50.4
−0.380	0.080	1.07	1109.5	53.1	−50.70	−20.01	3.63	−34.31	0.56	3.96	4.47	48.9
−0.380	0.080	1.08	1111.1	53.6	−51.12	−20.03	3.63	−34.73	0.56	3.96	4.47	45.9
−0.380	0.080	1.09	1112.8	54.0	−51.56	−20.04	3.63	−35.15	0.56	3.96	4.47	53.2
−0.380	0.080	1.10	1114.5	54.4	−51.99	−20.06	3.64	−35.57	0.56	3.96	4.47	57.9

[a]Density ρ, heat of vaporization ΔH_{vap}, potential energy U^{pot} with its Coulomb plus reaction-field (U^{CRF}), COS self-polarization ($U^{self-pol}$), and Lennard–Jones (U^{LJ}) contributions, molecular dipole μ^{ind}, the permanent molecular dipole μ^0, molecular dipole μ, static dielectric permittivity $\varepsilon(0)$. Angular brackets indicate averaging over molecules.

linearly between the pure liquids. The free enthalpy of hydrophobic solvation is for all three mixtures in the expected range. The induced dipole moment of the polarizable DMSO molecules is stable in the mixtures with polarizable and nonpolarizable water and with nonpolarizable DMSO. With increasing the amount of polarizable water, the induced dipole moment of the COS/G2 molecules is increasing linearly. The dielectric permittivity of DMSO–water mixtures in Figure 5 is not following the experimental trend for both of the water models. The simulations show no change in dielectric permittivity from the level for pure DMSO up until a water content of around 70%. Experimentally, an opposite trend is observed: beyond 30% water content the dielectric permittivity is almost that of pure water. For the mixtures of polarizable and

dx.doi.org/10.1021/jp5035695 | J. Phys. Chem. B 2014, 118, 10175–10186

Table 10. Properties of the DMSO Models with Polarizability α = 0.0045 $(4\pi\varepsilon_0)$ nm^3 and Damping with E_0 = 26 (kJ mol^{-1} nm^{-3})$^{1/2}$[a]

$f(C_{12})$	ρ	H_{vap}	U^{pot}	U^{CRF}	$U^{self-pol}$	U^{LJ}	$\langle\mu^{ind}\rangle$	μ^0	$\langle\mu\rangle$	$\varepsilon(0)$
	kg m^{-3}	kJ mol^{-1}	kJ mol^{-1}	kJ mol^{-1}	kJ mol^{-1}	kJmol^{-1}	D	D	D	
1.01	1107.4	53.7	−51.24	−19.50	3.41	−35.15	0.52	3.96	4.43	50.3
1.02	1101.7	53.2	−50.77	−19.39	3.39	−34.76	0.52	3.96	4.43	48.8
1.03	1095.8	52.7	−50.30	−19.29	3.36	−34.37	0.52	3.96	4.43	48.6
1.04	1090.2	52.3	−49.85	−19.19	3.33	−33.99	0.52	3.96	4.43	48.9
1.05	1084.7	51.9	−49.41	−19.09	3.30	−33.63	0.52	3.96	4.43	47.0

[a]The charge distribution is chosen to be q_O = −0.38 e, q_S = 0.08 e and q_C = 0.15 e and the Lennard−Jones ε_{LJ} parameter is multiplied by 1.1 for different scaling factors $f(C_{12})$ of the repulsive C_{12} Lennard−Jones parameter for all atom pairs. Density ρ, heat of vaporization ΔH_{vap}, potential energy U^{pot} with its Coulomb plus reaction-field (U^{CRF}), COS self-polarization ($U^{self-pol}$), and Lennard−Jones (U^{LJ}) contributions, induced molecular dipole μ^{ind}, the permanent molecular dipole μ^0, total molecular dipole μ, static dielectric permittivity $\varepsilon(0)$. Angular brackets indicate averaging over molecules.

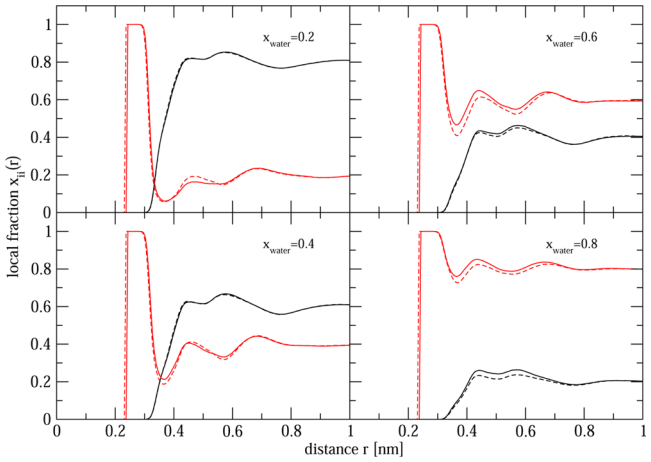

Figure 1. Local mole fractions $x_{ii}(r)$ for different binary mixtures of polarizable DMSO/D (black) and water (red). The binary mixture with polarizable COS/G2 water is shown as solid lines and the mixture with nonpolarizable SPC water as dashed lines.

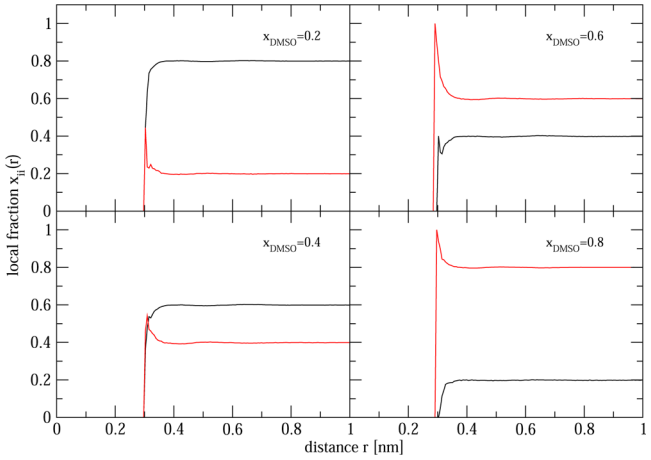

Figure 2. Local mole fractions $x_{ii}(r)$ for different binary mixtures of polarizable (DMSO/D, black) and nonpolarizable (DMSO, red) DMSO.

nonpolarizable DMSO, the dielectric permittivity is decreasing upon increasing the amount of polarizable DMSO molecules. The Debye relaxation time for the mixture of DMSO with water (Figure 5) shows a maximum around a mole fraction of $x_{COS/G2}$ = 0.6 for the mixture with polarizable water and x_{SPC} = 0.4−0.5 for nonpolarizable water.

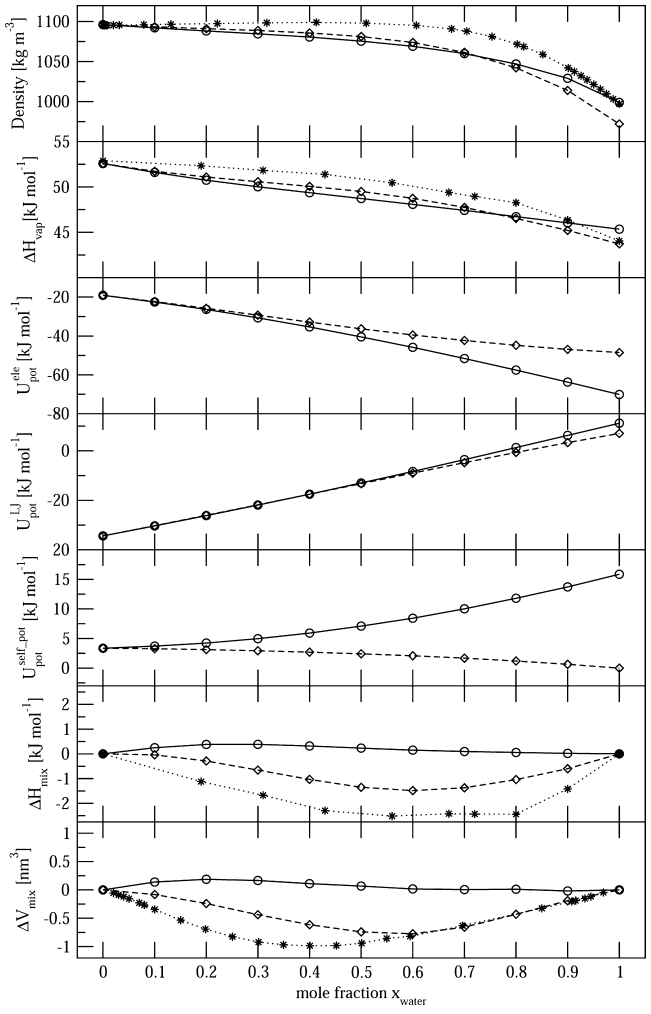

Figure 3. Density and energy per molecule for mixtures of polarizable DMSO/D and two different water models: polarizable COS/G2 (solid lines and circles) and nonpolarizable SPC (dashed lines and diamonds). The experimental results for the binary mixtures are represented by stars and a dotted line. x_{water} is the mole fraction of the water molecules in the mixtures. Density (ref 83). ΔH_{vap} = heat of vaporization (ref 84). U^{ele}_{pot} = electrostatic (Coulomb and reaction-field) energy. U^{LJ}_{pot} = Lennard−Jones interaction energy. $U^{self-pol}_{pot}$ = self-polarization energy. ΔH_{mix} = change of enthalpy upon mixing (ref 84). ΔV_{mix} = change of volume upon mixing (ref 85).

The dynamic and secondary thermodynamic properties for the mixtures of DMSO with water are shown in Figures 7 and 8

dx.doi.org/10.1021/jp5035695 | J. Phys. Chem. B 2014, 118, 10175−10186

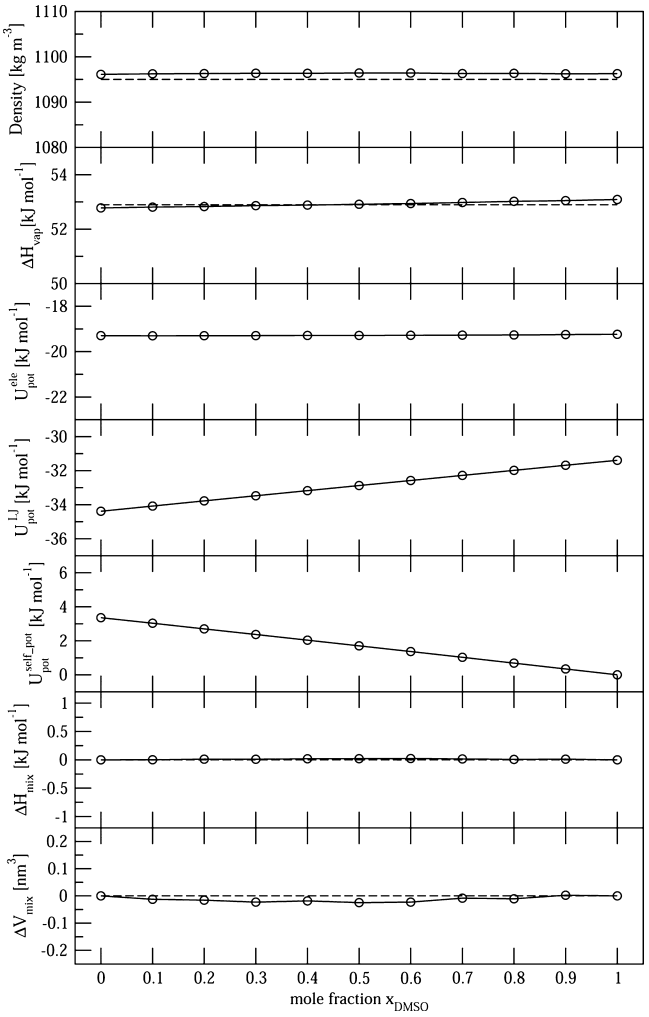

Figure 4. Density and energy per molecule for mixtures of polarizable DMSO/D and nonpolarizable DMSO molecules. x_{DMSO} is the mole fraction of nonpolarizable DMSO molecules. ΔH_{vap} = heat of vaporization. U_{pot}^{ele} = electrostatic (Coulomb and reaction-field) energy. U_{pot}^{LJ} = Lennard–Jones interaction energy. $U_{pot}^{self-pol}$ = self-polarization energy. ΔH_{mix} = change of enthalpy upon mixing. ΔV_{mix} = change of volume upon mixing. Horizontal dashed lines represent experimental (upper two panels) or ideal (lower two panels) values.

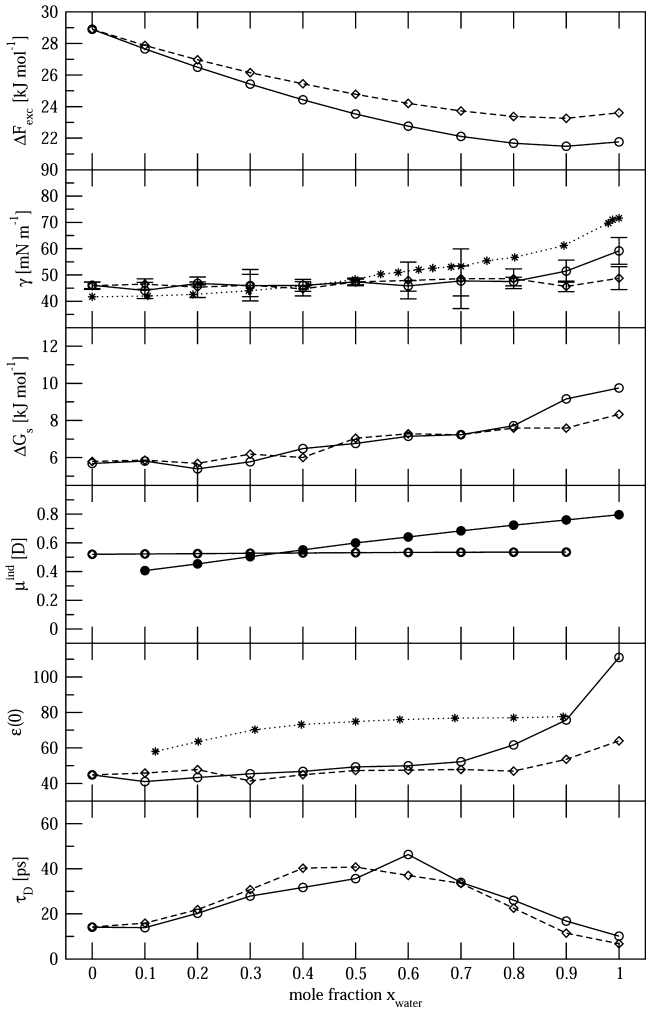

Figure 5. Free energies and dielectric properties for mixtures of polarizable DMSO/D with polarizable COS/G2 water (solid lines and circles) or with nonpolarizable SPC (dashed lines and diamonds) water. x_{water} is the mole fraction of water molecules. The experimental values are represented as dotted lines with stars. ΔF_{exc} = excess free energy of the liquid. γ = surface tension (ref 86). ΔG_s = free enthalpy of hydrophobic solvation. μ^{ind} = induced dipole moment (for COS/G2 molecules filled circles). $\varepsilon(0)$ = dielectric permittivity calculated from the fluctuating box dipole moment (ref 87). τ_D = Debye relaxation time. Horizontal dashed lines represent experimental values.

for the mixtures of polarizable with nonpolarizable DMSO molecules. The mixtures of polarizable DMSO and COS/G2 reproduce the experimental values for the diffusion of the DMSO and the water molecules. The mixtures of nonpolarizable SPC with polarizable DMSO show the same trend, reflecting the too fast diffusion of SPC molecules for high mole fractions of water. The translational and rotational diffusion of DMSO molecules in the mixtures of polarizable and nonpolarizable DMSO is roughly similar for all mole fractions. The mixtures of polarizable DMSO with nonpolarizable water show some longer relaxation times than for polarizable COS/G2 water mixed with polarizable DMSO. In general mixing DMSO and water slows down the rotation of both molecules, in particular water. The experimental values for the heat capacity show a linear decrease in DMSO-water mixtures. This trend is also observed for both water models but is less strong. The thermal expansion coefficients in Figure 7 for the DMSO–water mixtures are not reproducing the experimental data for high mole fractions of water due to the overestimation of the thermal expansion coefficient by the SPC and COS/G2 models. The isothermal compressibility in both DMSO-water mixtures shows a trend opposite to experiment. The mixtures are too compressible, which may be due to their slightly too low density (Figure 3). For the mixtures of polarizable DMSO/D and nonpolarizable DMSO molecules (Figure 8) the heat capacity, thermal expansion and compressibility show smooth behavior as a function of mole fraction.

DISCUSSION

When introducing polarizable sites into a model for a particular molecule, the number and spatial distribution over the molecule of the sites will determine how well the actual polarizability of the electron distribution of the molecule can be approximated. Since the computational effort rapidly grows with the number of sites, and since there are generally many solvent or cosolvent molecules present in a biomolecular simulation, it was decided to use only one polarizable site per

dx.doi.org/10.1021/jp5035695 | J. Phys. Chem. B 2014, 118, 10175–10186

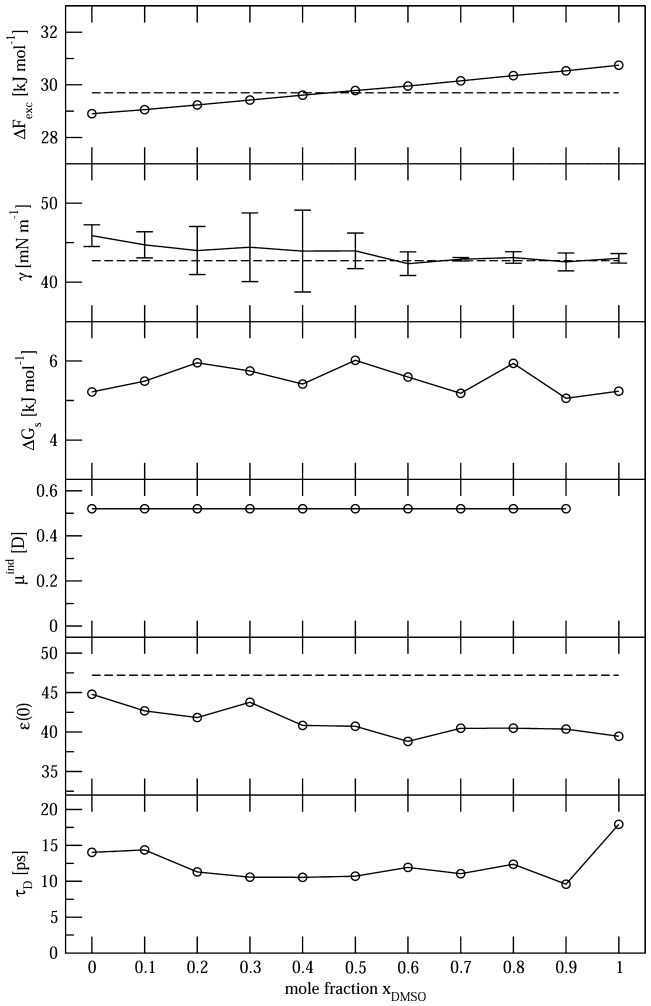

Figure 6. Free energies and dielectric properties for mixtures of polarizable DMSO/D and nonpolarizable DMSO molecules. x_{DMSO} is the mole fraction of nonpolarizable DMSO molecules. ΔF_{exc} = excess free energy of the liquid. γ = surface tension. ΔG_s = free enthalpy of hydrophobic solvation. μ^{ind} = induced dipole moment per DMSO/D molecule. $\varepsilon(0)$ = dielectric permittivity calculated from the fluctuating box dipole moment. τ_D = Debye relaxation time. Horizontal dashed lines represent experimental values.

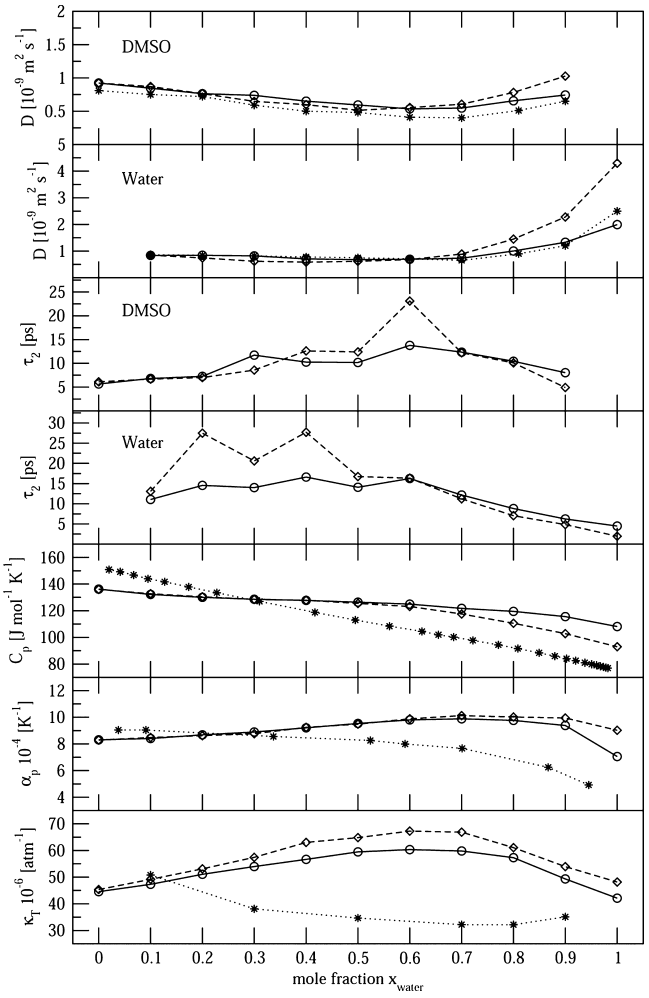

Figure 7. Dynamic and secondary thermodynamic properties for mixtures of polarizable DMSO/D and water: polarizable COS/G2 (solid lines and circles) and nonpolarizable SPC (dashed lines and diamonds) water. x_{water} is the mole fraction of water molecules in the binary mixtures. The experimental values are represented as dotted lines and stars. D = diffusion constant for the DMSO and water molecules (ref 88). τ_2 = second-order rotational correlation time of the S—O bond for DMSO and of the O—H bond for water. C_p = heat capacity per molecule at constant pressure (ref 89). α_p = thermal expansion coefficient (ref 90). κ_T = isothermal compressibility (ref 91).

DMSO molecule. This choice had the additional advantage of limiting the number of parameters in the model for which a value had to be chosen. The computational effort was increased by about a factor of 2.5 compared to the nonpolarizable DMSO model.

One may ask whether this increased computational effort is offset by improved properties of the polarizable DMSO/D model compared to the nonpolarizable DMSO models. The data in Table 2 show that the nonpolarizable DMSO model of ref 50 and the polarizable DMSO/D model perform overall equally well, with the latter having a better dielectric permittivity, a quantity that is of importance in biomolecular simulations. The mixing behavior of polarizable DMSO/D with polarizable COS/G2 water is worse than that when combining nonpolarizable DMSO of ref 50 with nonpolarizable SPC water, see ref 65. This is due to the too strong interaction between COS/G2 water molecules. Tests of the behavior of DMSO/D in combination with a new polarizable COS/D2 water model under development are in progress.

We note that the DMSO/D model and the nonpolarizable DMSO model of ref 50 show equal or better overall performance compared to other DMSO models for which properties are reported in the literature. The model of ref 47 is very similar to that of ref 50 and thus yields similar agreement with experiment with a too low dielectric permittivity. The properties reported for the model of ref 54 agree less with experiment than those obtained in ref 50. The model of ref 50 performs better on almost all counts than the model of ref 45. Yet, the models evaluated here are still not perfect. Although the introduction of polarizability enhance the computational effort, the better representation of the molecular polarizability and dielectric permittivity of the liquid may justify the use of the DMSO/D model for solvents of biomolecules.

■ CONCLUSIONS

A polarizable model for liquid DMSO that can be used in conjunction with GROMOS biomolecular force fields is

dx.doi.org/10.1021/jp5035695 | J. Phys. Chem. B 2014, 118, 10175−10186

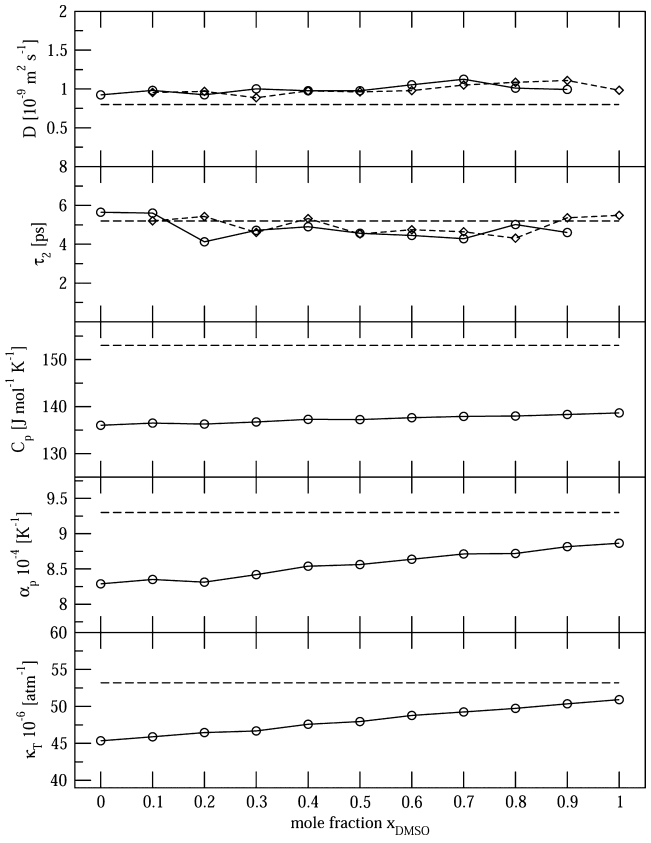

Figure 8. Dynamic and secondary thermodynamic properties for mixtures of polarizable DMSO/D and nonpolarizable DMSO molecules. x_{DMSO} is the mole fraction of nonpolarizable DMSO molecules. D = diffusion constant of DMSO/D (solid lines and circles) and DMSO (dashed lines and diamonds). τ_2 = second-order rotational correlation time of the S—O bond for DMSO/D (solid lines and circles) and DMSO (dashed lines and diamonds) molecules. C_p = heat capacity per molecule at constant pressure. α_p = thermal expansion coefficient. κ_T = isothermal compressibility. Horizontal long dashed lines represent experimental values.

proposed. It is based on the charge-on-spring (COS) representation of polarizability using one COS site on the sulfur atom. Because the DMSO molecules, even with the CH_3 groups represented as united atoms, still has four atoms and three atom types, S, O, and CH_3, a molecular model for DMSO based on electrostatic and van der Waals interactions has too many parameters to allow for an investigation of all possible combinations of parameter values at a reasonable computational effort. Therefore, the nonpolarizable DMSO model of ref 50 was chosen as starting point for the parameter calibration of the polarizable DMSO model. The DMSO/D model shows as good agreement with experimental data for DMSO in the condensed phase as the nonpolarizable DMSO model of ref 50 with an improved dielectric permittivity. The properties of DMSO/D-water mixtures using a polarizable model (COS/G2) and a nonpolarizable model (SPC) for water are reproduced except for the observed slightly nonideal behavior of these mixtures, which seems to be due to the COS/G2 polarizable water model that shows larger deviations from experiment for properties such as the excess free energy, surface tension, and dielectric permittivity, than the DMSO/D polarizable model for DMSO. The polarizable DMSO/D model is compatible with the nonpolarizable DMSO model of ref 50, which indicates that it may be used in mixtures of molecules modeled with or without explicit molecular polarizability.

AUTHOR INFORMATION

Corresponding Author

*E-mail: wfvgn@igc.phys.chem.ethz.ch.

Notes

The authors declare no competing financial interest.

ACKNOWLEDGMENTS

This work was financially supported by the National Center of Competence in Research (NCCR) in Structural Biology and by Grant Number 200020-137827 of the Swiss National Science Foundation, and by Grant Number 228076 of the European Research Council, which is gratefully acknowledged.

REFERENCES

(1) Scheraga, H. A.; Khalili, M.; Liwo, A. Protein-Folding Dynamics: Overview of Molecular Simulation Techniques. *Annu. Rev. Phys. Chem.* **2007**, *58*, 57−83.

(2) Lindahl, E.; Sansom, M. S. P. Membrane Proteins: Molecular Dynamics Simulations. *Curr. Opin. Struct. Biol.* **2008**, *18*, 425−431.

(3) Khalili-Araghi, F.; Gumbart, J.; Wen, P.-C.; Sotomayor, M.; Tajkhorshid, E.; Schulten, K. Molecular Dynamics Simulations of Membrane Channels and Transporters. *Curr. Opin. Struct. Biol.* **2009**, *19*, 128−137.

(4) van Gunsteren, W. F.; Dolenc, J. Thirty-Five Years of Biomolecular Simulation: Development of Methodology, Force Fields and Software. *Mol. Sim.* **2012**, *38*, 1271−1281.

(5) van Gunsteren, W. F.; Bakowies, D.; Baron, R.; Chandrasekhar, I.; Christen, M.; Daura, X.; Gee, P.; Geerke, D. P.; Glättli, A.; Hünenberger, P. H.; et al. Biomolecular Modeling: Goals, Problems, Perspectives. *Angew. Chem., Int. Ed.* **2006**, *45*, 4064−4092.

(6) Brooks, B. R.; Bruccoleri, R. E.; Olafson, B. D.; States, D. J.; Swaminathan, S.; Karplus, M. CHARMM: A Program for Macromolecular Energy, Minimization, and Dynamics Calculations. *J. Comput. Chem.* **1983**, *4*, 187−217.

(7) MacKerell, A. D.; Bashford, D.; Bellott; Dunbrack, R. L.; Evanseck, J. D.; Field, M. J.; Fischer, S.; Gao, J.; Guo, H.; Ha, S.; et al. All-Atom Empirical Potential for Molecular Modeling and Dynamics Studies of Proteins. *J. Phys. Chem. B* **1998**, *102*, 3586−3616.

(8) Weiner, P. K.; Kollman, P. A. AMBER: Assisted Model Building with Energy Refinement. A General Program for Modeling Molecules and Their Interactions. *J. Comput. Chem.* **1981**, *2*, 287−303.

(9) Cornell, W. D.; Cieplak, P.; Bayly, C. I.; Gould, I. R.; Merz, K. M.; Ferguson, D. M.; Spellmeyer, D. C.; Fox, T.; Caldwell, J. W.; Kollman, P. A. A Second Generation Force Field for the Simulation of Proteins, Nucleic Acids, and Organic Molecules. *J. Am. Chem. Soc.* **1995**, *117*, 5179−5197.

(10) van Gunsteren, W. F.; Karplus, M. Effect of Constraints, Solvent and Crystal Environment on Protein Dynamics. *Nature* **1981**, *293*, 677−678.

(11) Schmid, N.; Eichenberger, A. P.; Choutko, A.; Riniker, S.; Winger, M.; Mark, A. E.; van Gunsteren, W. F. Definition and Testing of the GROMOS Force-Field Versions 54A7 and 54B7. *Eur. Biophys. J.* **2011**, *40*, 843−856.

(12) Jorgensen, W. L.; Tirado-Rives, J. The OPLS [Optimized Potentials for Liquid Simulations] Potential Functions for Proteins, Energy Minimizations for Crystals of Cyclic Peptides and Crambin. *J. Am. Chem. Soc.* **1988**, *110*, 1657−1666.

(13) Jorgensen, W. L.; Maxwell, D. S.; Tirado-Rives, J. Development and Testing of the OPLS All-Atom Force Field on Conformational Energetics and Properties of Organic Liquids. *J. Am. Chem. Soc.* **1996**, *118*, 11225−11236.

(14) Kirchner, B.; Reiher, M. The Secret of Dimethyl Sulfoxide−Water Mixtures. A Quantum Chemical Study of $1DMSO_n^-$ Water Clusters. *J. Am. Chem. Soc.* **2002**, *124*, 6206−6215.

(15) Rick, S. W.; Stuart, S. J. In *Potentials and Algorithms for Incorporating Polarizability in Computer Simulations*; John Wiley & Sons, Inc.: New York, 2002; Chapter 8, pp 89−146.
(16) Yu, H.; van Gunsteren, W. F. Accounting for Polarization in Molecular Simulation. *Comput. Phys. Commun.* **2005**, *172*, 69−85.
(17) Warshel, A.; Levitt, M. Theoretical Studies of Enzymic Reactions—Dielectric, Electrostatic and Steric Stabilization of Carbonium-Ion in Reaction of Lysozyme. *J. Mol. Biol.* **1976**, *103*, 227−249.
(18) Vesely, F. J. N-Particle Dynamics of Polarizable Stockmayer-Type Molecules. *J. Comput. Phys.* **1977**, *24*, 361−371.
(19) van Belle, D.; Couplet, I.; Prevost, M.; Wodak, S. J. Calculations of Electrostatic Properties in Proteins: Analysis of Contributions from Induced Protein Dipoles. *J. Mol. Biol.* **1987**, *198*, 721−735.
(20) Rick, S. W.; Stuart, S. J.; Berne, B. J. Dynamical Fluctuating Charge Force Fields: Application to Liquid Water. *J. Chem. Phys.* **1994**, *101*, 6141−6156.
(21) Straatsma, T. P.; McCammon, J. A. Molecular Dynamics Simulations with Interaction Potentials Including Polarization Development of a Noniterative Method and Application to Water. *Mol. Sim.* **1990**, *5*, 181−192.
(22) Drude, P. *The Theory of Optics*; Longmans, Green, and Co.: London, 1902.
(23) Huang, K.; Born, M. *Dynamic Theory of Crystal Lattices*; Oxford University Press: Oxford, U.K., 1984.
(24) Kunz, A.-P. E.; Allison, J. R.; Geerke, D. P.; Horta, B. A. C.; Hünenberger, P. H.; Riniker, S.; Schmid, N.; van Gunsteren, W. F. New Functionalities in the GROMOS Biomolecular Simulation Software. *J. Comput. Chem.* **2012**, *33*, 340−353.
(25) Bachmann, S. J.; van Gunsteren, W. F. On the Compatibility of Polarisable and Non-Polarisable Models for Liquid Water. *Mol. Phys.* **2014**.
(26) van Gunsteren, W. F.; Bürgi, R.; Peter, C.; Daura, X. The Key to Solving the Protein-Folding Problem Lies in an Accurate Description of the Denatured State. *Angew. Chem., Int. Ed.* **2001**, *40*, 351−355.
(27) van Gunsteren, W. F.; Bürgi, R.; Peter, C.; Daura, X. Reply to the Comment on the Communication by van Gunsteren et al., *Angew. Chem. Int. Ed. 40* (**2001**) 351−355. *Angew. Chem., Int. Ed.* **2001**, *40*, 4616−4618.
(28) Fuchs, R.; McCrary, G. E.; Bloomfield, J. J. Mechanisms of Nucleophilic Displacement in Aqueous Dimethyl Sulfoxide Solutions. *J. Am. Chem. Soc.* **1961**, *83*, 4281−4284.
(29) Safford, G. J.; Schaffer, P. C.; Leung, P. S.; Doebbler, G. F.; Brady, G. W.; Lyden, E. F. X. Neutron Inelastic Scattering and X-Ray Studies of Aqueous Solutions of Dimethylsulfoxide and Dimethylsulphone. *J. Chem. Phys.* **1969**, *50*, 2140−2159.
(30) Brink, G.; Falk, M. The Effect of Dimethyl Sulfoxide on the Structure of Water. *J. Mol. Sruct.* **1970**, *5*, 27−30.
(31) Packer, K. J.; Tomlinson, D. J. Nuclear Spin Relaxation and Self-Diffusion in the Binary System, Dimethylsulfoxide $(DMSO)^{+}$ Water. *Trans. Faraday Soc.* **1971**, *67*, 1302−1314.
(32) Tokuhiro, T.; Menafra, L.; Szmant, H. H. Contribution of Relaxation and Chemical Shift Results to the Elucidation of the Structure of the Water−DMSO Liquid System. *J. Chem. Phys.* **1974**, *61*, 2275−2282.
(33) Fox, M. F.; Whittingham, K. P. Component Interactions in Aqueous Dimethyl Sulfoxide. *J. Chem. Soc., Faraday Trans. 1* **1975**, *71*, 1407−1412.
(34) Bertoluzza, A.; Bonora, S.; Battaglia, M. A.; Monti, P. Raman and Infrared Study on the Effects of Dimethylsulfoxide (DMSO) on Water Structure. *J. Raman Spectrosc.* **1979**, *8*, 231−235.
(35) Madigosky, W. M.; Warfield, R. W. Ultrasonic Measurements and Liquid Structure of DMSO−Water Mixture. *J. Chem. Phys.* **1983**, *78*, 1912−1916.
(36) Kaatze, U.; Pottel, R.; Schaefer, M. Dielectric Spectrum of Dimethyl Sulfoxide/Water Mixtures as a Function of Composition. *J. Phys. Chem.* **1989**, *93*, 5623−5627.
(37) Baker, E. S.; Jonas, J. Transport and Relaxation Properties of Dimethyl Sulfoxide−Water Mixtures at High Pressure. *J. Phys. Chem.* **1985**, *89*, 1730−1735.
(38) Gordalla, B. C.; Zeidler, M. D. NMR Proton Relaxation and Chemical Exchange in the System $H^{16}{}_2O/H^{17}{}_2O^{-}[^2H_6]$-Simethylsulfoxide. *Mol. Phys.* **1991**, *74*, 975−984.
(39) Luzar, A.; Soper, A. K.; Chandler, D. Combined Neutron Diffraction and Computer simulation study of liquid dimethyl sulfoxide. *J. Chem. Phys.* **1993**, *99*, 6836−6847.
(40) Ludwig, R.; Farrar, T. C.; Zeidler, M. D. Temperature Dependence of the Deuteron and Oxygen Quadrupole Coupling Constants of Water in the System Water/Dimethyl Sulfoxide. *J. Phys. Chem.* **1994**, *98*, 6684−6687.
(41) Lai, J. T. W.; Lau, F. W.; Robb, D.; Westh, P.; Nielsen, G.; Trandum, C.; Hvidt, A.; Koga, Y. Excess Partial Molar Enthalpies, Entropies, Gibbs Energies, and Volumes in Aqueous Dimethylsulfoxide. *J. Solution Chem.* **1995**, *24*, 89−102.
(42) Mancera, R. L.; Chalaris, M.; Samios, J. The Concentration Effect on the Hydrophobic and Hydrophilic Behaviour Around DMSO in Dilute Aqueous DMSO Solutions. A Computer Simulation Study. *J. Mol. Liq.* **2004**, *110*, 147−153.
(43) Mancera, R. L.; Chalaris, M.; Refson, K.; Samios, J. Molecular Dynamics Simulation of Dilute Aqueous DMSO Solutions. A Temperature-Dependence Study of the Hydrophobic and Hydrophilic Behaviour Around DMSO. *Phys. Chem. Chem. Phys.* **2004**, *6*, 94−102.
(44) Zhang, Q.; Zhang, X.; Zhao, D.-X. Polarizable Force Field for Water−Dimethyl Sulfoxide Systems: I Parameterization and Gas Phase Test. *J. Mol. Liq.* **2009**, *145*, 58−66.
(45) Zhang, Q.; Zhang, X.; Zhao, D.-X. Polarizable Force Field for Water−Dimethyl Sulfoxide Systems: II Properties of Mixtures by Molecular Dynamics Simulations. *J. Mol. Liq.* **2009**, *145*, 67−81.
(46) Rao, B. G.; Singh, U. C. A Free Energy Perturbation Study of Solvation in Methanol and Dimethyl Sulfoxide. *J. Am. Chem. Soc.* **1990**, *112*, 3803−3811.
(47) Liu, H.; Mueller-Plathe, F.; van Gunsteren, W. F. A Force Field for Liquid Dimethyl Sulfoxide and Physical Properties of Liquid Dimethyl Sulfoxide Calculated Using Molecular Dynamics Simulation. *J. Am. Chem. Soc.* **1995**, *117*, 4363−4366.
(48) Vishnyakov, A.; Lyubartsev, A. P.; Laaksonen, A. Molecular Dynamics Simulations of Dimethyl Sulfoxide and Dimethyl Sulfoxide-Water Mixture. *J. Phys. Chem. A* **2001**, *105*, 1702−1710.
(49) Bordat, P.; Sacristan, J.; Reith, D.; Girard, S.; Glättli, A.; Müller-Plathe, F. An Improved Dimethyl Sulfoxide Force Field for Molecular Dynamics Simulations. *Chem. Phys. Lett.* **2003**, *374*, 201−205.
(50) Geerke, D. P.; Oostenbrink, C.; van der Vegt, N. F. A.; van Gunsteren, W. F. An Effective Force Field for Molecular Dynamics Simulations of Dimethyl Sulfoxide and Dimethyl Sulfoxide−Water Mixtures. *J. Phys. Chem. B* **2004**, *108*, 1436−1445.
(51) Chalaris, M.; Marinakis, S.; Dellis, D. Temperature Effects on the Structure and Dynamics of Liquid Dimethyl Sulfoxide: A Molecular Dynamics Study. *Fluid Phase Equilib.* **2008**, *267*, 47−60.
(52) Fox, T.; Kollman, P. A. Application of the RESP Methodology in the Parametrization of Organic Solvents. *J. Phys. Chem. B* **1998**, *102*, 8070−8079.
(53) Benjamin, I. Structure, Thermodynamics, and Dynamics of the Liquid/Vapor Interface of Water/Dimethylsulfoxide Mixtures. *J. Chem. Phys.* **1999**, *110*, 8070−8079.
(54) Strader, M. L.; Feller, S. E. A Flexible All-Atom Model of Dimethyl Sulfoxide for Molecular Dynamics Simulations. *J. Phys. Chem. A* **2002**, *106*, 1074−1080.
(55) Senapati, S. A Molecular Dynamics Simulation Study of the Dimethyl Sulfoxide Liquid−Vapor Interface. *J. Chem. Phys.* **2002**, *117*, 1812−1816.
(56) Allison, J. R.; Riniker, S.; van Gunsteren, W. F. Coarse-Grained Models for the Solvents Dimethyl Sulfoxide, Chloroform, and Methanol. *J. Chem. Phys.* **2012**, *136*, 054505.
(57) Yu, H.; van Gunsteren, W. F. Charge-on-Spring Polarizable Water Models Revisited: From Water Clusters to Liquid Water to Ice. *J. Chem. Phys.* **2004**, *121*, 9549−9564.
(58) van Gunsteren, W. F.; Billeter, S. R.; Eising, A. A.; Hünenberger, P. H.; Krüger, P.; Mark, A. E.; Scott, W. R. P.; Tironi, I. *Biomolecular*

Simulation: The GROMOS96 Manual and User Guide; Vdf Hochschulverlag AG an der ETH Zürich: Zürich, 1996.
(59) Christen, M.; Hünenberger, P. H.; Bakowies, D.; Baron, R.; Bürgi, R.; Geerke, D. P.; Heinz, T. N.; Kastenholz, M. A.; Kräutler, V.; Oostenbrink, C.; et al. The GROMOS Software for Biomolecular Simulation: GROMOS05. *J. Comput. Chem.* **2005**, *26*, 1719−1751.
(60) van Gunsteren, W. F. www.gromos.net, (accessed 27/03/2014).
(61) Ryckaert, J.-P.; Ciccotti, G.; Berendsen, H. J. C. Numerical Integration of the Cartesian Equations of Motion of a System with Constraints: Molecular Dynamics of n-Alkanes. *J. Comput. Phys.* **1977**, *23*, 327−341.
(62) Barker, J. A.; Watts, R. O. Monte Carlo Studies of the Dielectric Properties of Water-Like Models. *Mol. Phys.* **1973**, *26*, 789−792.
(63) Tironi, I. G.; Sperb, R.; Smith, P. E.; van Gunsteren, W. F. A Generalized Reaction Field Method for Molecular Dynamics Simulations. *J. Chem. Phys.* **1995**, *102*, 5451−5459.
(64) Berendsen, H. J. C.; Postma, J. P. M.; van Gunsteren, W. F.; DiNola, A.; Haak, J. R. Molecular Dynamics with Coupling to an External Bath. *J. Chem. Phys.* **1984**, *81*, 3684−3690.
(65) Berendsen, H. J. C.; Postma, J. P. M.; van Gunsteren, W. F.; Hermans, J. Interaction Models for Water in Relation to Protein Hydration. In *Intermolecular Forces*; Pullman, B., Ed.; Reidel: Dordrecht, The Netherlands, 1981; pp 331−342.
(66) Miller, K. J. Additivity Methods in Molecular Polarizability. *J. Am. Chem. Soc.* **1990**, *112*, 8533−8542.
(67) Kunz, A.-P. E.; van Gunsteren, W. F. Development of a Nonlinear Classical Polarization Model for Liquid Water and Aqueous Solutions: COS/D. *J. Phys. Chem. A* **2009**, *113*, 11570−11579.
(68) Riddick, J. A.; Buger, W. B.; Sakand, T. K. *Organic Solvents: Physical Properties and Methods of Purification*; Wiley: New York, 1986.
(69) Kell, G. S. Precise Representation of Volume Properties of Water at One Atmosphere. *J. Chem. Eng. Data* **1967**, *12*, 66−69.
(70) Guillot, B. A Reappraisal of What We Have Learnt During Three Decades of Computer Simulations on Water. *J. Mol. Liq.* **2002**, *101*, 219−260.
(71) Hayward, J. A.; Reimers, J. R. Unit Cells for the Simulation of Hexagonal Ice. *J. Chem. Phys.* **1997**, *106*, 1518−1529.
(72) Hermans, J.; Pathiaseril, A.; Anderson, A. Excess Free Energy of Liquids from Molecular Dynamics Simulations. Application to Water Models. *J. Am. Chem. Soc.* **1988**, *110*, 5982−5986.
(73) Kinart, C. M.; Kinart, W. J.; Bald, A. The Measurements of the Surface Tension of Mixtures of Dimethyl Sulfoxide with Methyl, Ethyl, and Propyl Alcohols. *Phys. Chem. Liq.* **1999**, *37*, 317−321.
(74) Chen, F.; Smith, P. E. Simulated Surface Tensions of Common Water Models. *J. Chem. Phys.* **2007**, *126*, 221101.
(75) Ben-Naim, A.; Marcus, Y. Solvation Thermodynamics of Nonionic Solutes. *J. Chem. Phys.* **1984**, *81*, 2016−2027.
(76) Lide, D. R. *Handbook of Chemistry and Physics*, 88th ed.; CRC PRESS/Taylor and Francis: Boca Raton, FL, 2007−2008.
(77) Shostak, S. L.; Ebenstein, W. L.; Muenter, J. S. The Dipole Moment of Water: Dipole Moments and Hyperfine Properties of H_2O and HDO in the Ground and Excited Vibrational States. *J. Chem. Phys.* **1991**, *94*, 5875−5882.
(78) Cebe, E.; Kaltenmeier, D.; Hertz, G. H. A Study Concerning Self-Association in Mixtures of Cyclohexane, Benzene and DMSO with CCl_4 by the Nuclear Magnetic Relaxation Method. *Z. Phys. Chem.* **1984**, *140*, 181−189.
(79) Krynicki, K.; Green, C. D.; Sawyer, D. W. Pressure and Temperature Dependence of Self-Diffusion in Water. *Faraday Discuss. Chem. Soc.* **1978**, *66*, 199−208.
(80) Kovacs, H.; Kowalewski, J.; Maliniak, A. Sulfur-33 Rleaxation and Nuclear Quadrupole Coupling Constant in Dimethylsulfoxide. *Acta. Chem. Scand. A* **1987**, *41*, 471−479.
(81) Ludwig, R. NMR Relaxation Studies in Water−Alcohol Mixtures: The Water-Rich Region. *Chem. Phys.* **1995**, *195*, 329−337.
(82) Motakabbir, K. A.; Berkowitz, M. Isothermal Compressibility of SPC/E Water. *J. Phys. Chem.* **1990**, *94*, 8359−8362.
(83) Egorov, G.; Makarov, D. The Bulk Properties of the Water−Dimethylsulfoxide System at 278−323.15 K and Atmospheric Pressure. *Russ. J. Phys. Chem. A* **2009**, *83*, 693−698.
(84) Cowie, J. M. G.; Toporowski, P. M. Assocation in the Binary Liquid System Dimethyl Sulfoxide−Water. *Can. J. Chem.* **1961**, *39*, 2240−2243.
(85) Torres, R. B.; Marchiore, A.; Volpe, P. Volumetric Properties of Binary Mixtures of (Water + Organic Solvents) at Temperatures between T = 288.15 K and T = 0; 303.15 K at p = 0.1 MPa. *J. Chem. Thermodyn.* **2006**, *38*, 526−541.
(86) Markarian, S. A.; Terzyan, A. M. Surface Tension and Refractive Index of Dialkylsulfoxide + Water Mixtures at Several Temperatures. *J. Chem. Eng. Data* **2007**, *52*, 1704−1709.
(87) Campbell, A. N.; Kartzmark, E. M. Conductivities of Lanthanum Chloride in Water−Dimethyl Sulfoxide Mixtures at 25 °C. *J. Chem. Eng. Data* **1984**, *29*, 168−171.
(88) Catalan, J.; Diaz, C.; Garcia-Blanco, F. Characterization of Binary Solvent Mixtures of DMSO with Water and Other Cosolvents. *J. Org. Chem.* **2001**, *66*, 5846−5852.
(89) Checoni, R.; Volpe, P. Measurements of the Molar Heat Capacities and Excess Molar Heat Capacities for Water + Organic Solvents Mixtures at 288.15 to 303.15 K and Atmospheric Pressure. *J. Solution Chem.* **2010**, *39*, 259−276.
(90) Markarian, S. A.; Asatryan, A. M.; Zatikyan, A. L. Volumetric Properties of Aqueous Solutions of Diethylsulfoxide at Temperatures from 298.15 to 343.15 K. *J. Chem. Thermodyn.* **2005**, *37*, 768−777.
(91) Syrbu, V. A.; Lupina, M. I.; Shakhparonov, M. I. Acoustic Spectra of Dimethyl Sulfoxide, Solutions of Dimethyl Sulfoxide—Water and Their Analysis. *Zh. Fiz. Khim.* **1977**, *51*, 800−804.